

AD 608027

AIR FORCE  
ASTIC MISSILE DIVISION

TECHNICAL LIBRARY

9-4790  
1

✓ B

1

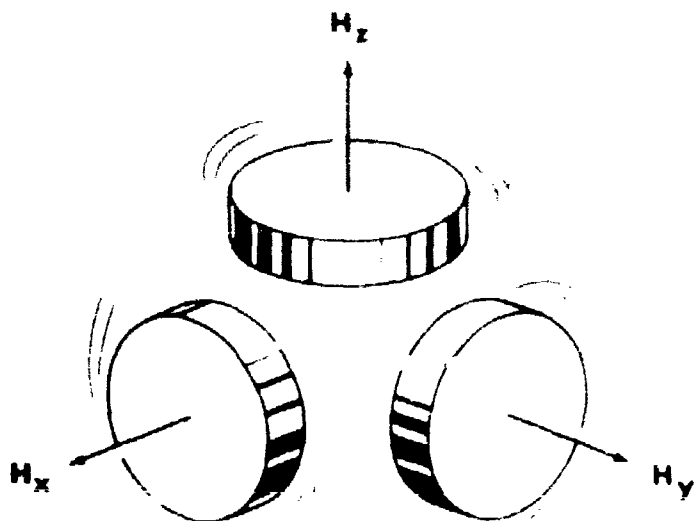
# REACTION WHEEL ATTITUDE CONTROL FOR SPACE VEHICLES

COPY	1	OF	1
HARD COPY			\$ .2.00
MICROFICHE			\$ .0.50

30p

Ronald W. Froelich  
Harry Potapoff

October 1959



ARCHIVE COPY

DDC  
NOV 4 - 1964

**Best  
Available  
Copy**

AD 608027

REACTION WHEEL ATTITUDE CONTROL  
FOR SPACE VEHICLES

by

Ronald W. Froelich and Harry Patapoff

To be presented at the  
IRE National Automatic Control Conference  
November 6, 1959  
Dallas, Texas

SPACE TECHNOLOGY LABORATORIES, INC.  
P. O. Box 95001  
Los Angeles 45, California

## SUMMARY

An attitude control system consisting of motor-driven inertial wheels in conjunction with an over-riding mass ejection system is proposed for use in space vehicles. Control by mass ejection is used to compensate for initial disturbances during separation from the booster, and for removal of unwanted momentum stored in the wheels. The use of reaction wheels permits fine, damped attitude control.

A laboratory model of a single-axis control system was constructed for experimentation and evaluation. The choice of a suitable platform configuration, selection of a prime mover for the inertial wheel, and the philosophy in the design of the electronics and pneumatics are discussed. Emphasis was placed upon minimization of weight and power consumption. System evaluation includes a discussion of efficiencies, reliability, and torque-speed-power relationships.

Sources of disturbances, methods of sensing, and general equations of motion are presented in the Appendix.

## SUMMARY

An attitude control system consisting of motor-driven inertial wheels in conjunction with an over-riding mass ejection system is proposed for use in space vehicles. Control by mass ejection is used to compensate for initial disturbances during separation from the booster, and for removal of unwanted momentum stored in the wheels. The use of reaction wheels permits fine, damped attitude control.

A laboratory model of a single-axis control system was constructed for experimentation and evaluation. The choice of a suitable platform configuration, selection of a prime mover for the inertial wheel, and the philosophy in the design of the electronics and pneumatics are discussed. Emphasis was placed upon minimization of weight and power consumption. System evaluation includes a discussion of efficiencies, reliability, and torque-speed-power relationships.

Sources of disturbances, methods of sensing, and general equations of motion are presented in the Appendix.

## CONTENTS

	Page
I. INTRODUCTION . . . . .	1
II. SYSTEM DESCRIPTION . . . . .	1
III. THE LABORATORY MODEL . . . . .	2
A. The Platform . . . . .	5
B. The Motor . . . . .	5
1. A-C Motors . . . . .	6
2. D-C Motors . . . . .	6
C. The Electronics . . . . .	8
1. A-C Motor Power Amplifier . . . . .	8
2. D-C Motor Power Amplifier . . . . .	11
a. Power System . . . . .	11
b. Commutation System . . . . .	13
3. Velocity Servo Loop . . . . .	13
D. The Sensor . . . . .	14
E. The Pneumatics . . . . .	15
IV. GENERAL . . . . .	15
A. Reliability . . . . .	15
B. Torque, Speed, Power Relationships . . . . .	15
C. Space Vehicle Control . . . . .	17
D. Design Consideration . . . . .	17
E. Selection of Control Equations . . . . .	17
APPENDIX . . . . .	19
A. Disturbance Sources . . . . .	19
B. Sensing Methods . . . . .	19
C. Equations of Motion . . . . .	20

## ILLUSTRATIONS

<u>Figure</u>		<u>Page</u>
1	Block Diagram of Laboratory Model of Single-Axis Control System . . . . .	3
2	Laboratory Model . . . . .	4
3	Block Diagram of A-C System . . . . .	9
4	Waveforms in Control Circuitry of A-C System . . . . .	10
5	Block Diagram of D-C Speed Control System . . . . .	12
6	Essential Waveforms in the D-C System . . . . .	12
7	Mechanics of Sensor . . . . .	14
8	Gas Solenoid and Sensor Mounted on Table . . . . .	16
9	Deviation Angles . . . . .	22

## I. INTRODUCTION

The use of inertial wheels is a feasible and relatively simple method for controlling the attitude of a space vehicle. A wide, continuous range of control torques is obtainable, permitting fine, damped attitude control. Furthermore, the generation of these control torques does not require any interaction with ambient fields, which vary with altitude and position. Control torques are derived by inertial means, and are therefore independent of the location of the vehicle.

The low weight requirement, low power consumption, and attainable reliability should make a reaction wheel control system appealing for future space programs. This is especially true in cases where precise attitude control is required for a long period of time, and where electrical energy is to be generated in flight by means of solar cells or nuclear power supplies.

An experimental laboratory model of a single-axis control system was constructed from off-the-shelf components employing several novel techniques in circuitry. The purpose of constructing such a model was to resolve major problems associated with the design and construction of logic circuitry, power amplifier, and prime mover, in order to obtain a system in which weight and power consumption are minimized. Insofar as practical, single-axis control of a space vehicle was simulated in order to evaluate performance and reliability.

Without employing a major research program, a practical three-dimensional reaction wheel attitude control system for a space vehicle can be constructed with only minor modifications of the system employed in the laboratory model.

## II. SYSTEM DESCRIPTION

A hybrid system consisting of a motor-driven inertial wheel and an auxiliary mass ejection system employing constant thrust gas jets is considered here. Cold pressurized helium is used for thrust generation.

The motor-driven wheel is mounted upon a platform suspended horizontally by means of knife edges. Angular deviations of the platform from the desired attitude are sensed, and the resulting error signals are used to accelerate the



wheel in the direction of the deviations. The reaction torque on the platform reduces these deviations to zero. Figure 1 shows a block diagram of the wheel system.

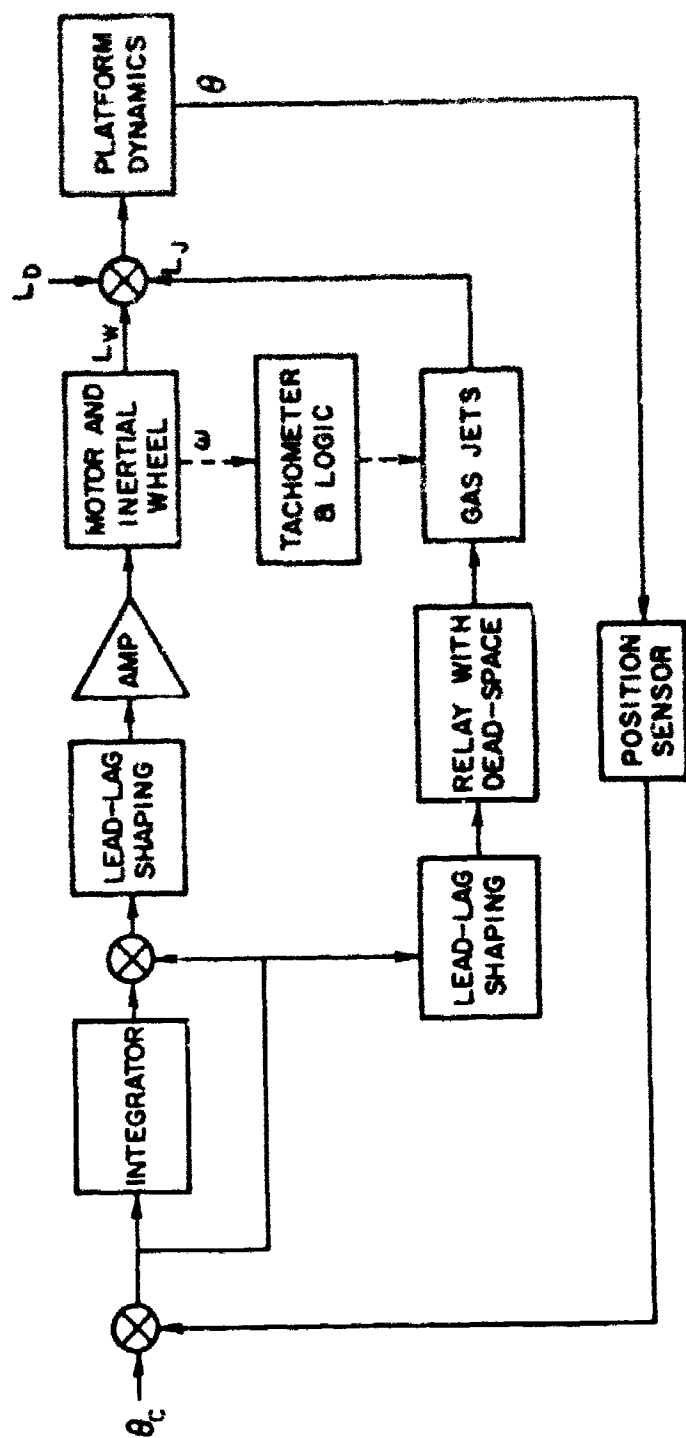
The reaction wheel system is in essence a momentum transfer and storage device, absorbing momentum from the platform. The steady-state behavior of the system in the presence of a constant disturbance torque is a constant acceleration of the wheel, whose reaction torque on the platform is equal and opposite to the disturbance. In the absence of disturbances, constant wheel speed is maintained.

The function of the pneumatic system is to remove undesired momentum from the vehicle or wheel. It is used to reduce any large angular rates imparted to the platform, and to insure that the inertial wheel speed is maintained below a pre-set level. This level is governed by the maximum speed of the motor and by power losses, which are a function of wheel speed. If the wheel speed exceeds this pre-set value, the tachometer activates the pneumatic system and sufficient impulse is generated to reduce the wheel speed. The system then reverts to wheel control.

A block diagram of the pneumatic system appears in Figure 1. The relay has a specified dead-space within which the reaction wheel system operates. The pneumatic system is also an over-riding system for the reaction wheels. If any large spurious disturbance should occur during wheel control, pneumatic control is initiated either when the attitude deviation exceeds the deviation corresponding to the relay dead-space value, or when the platform angular rate becomes sufficiently large.

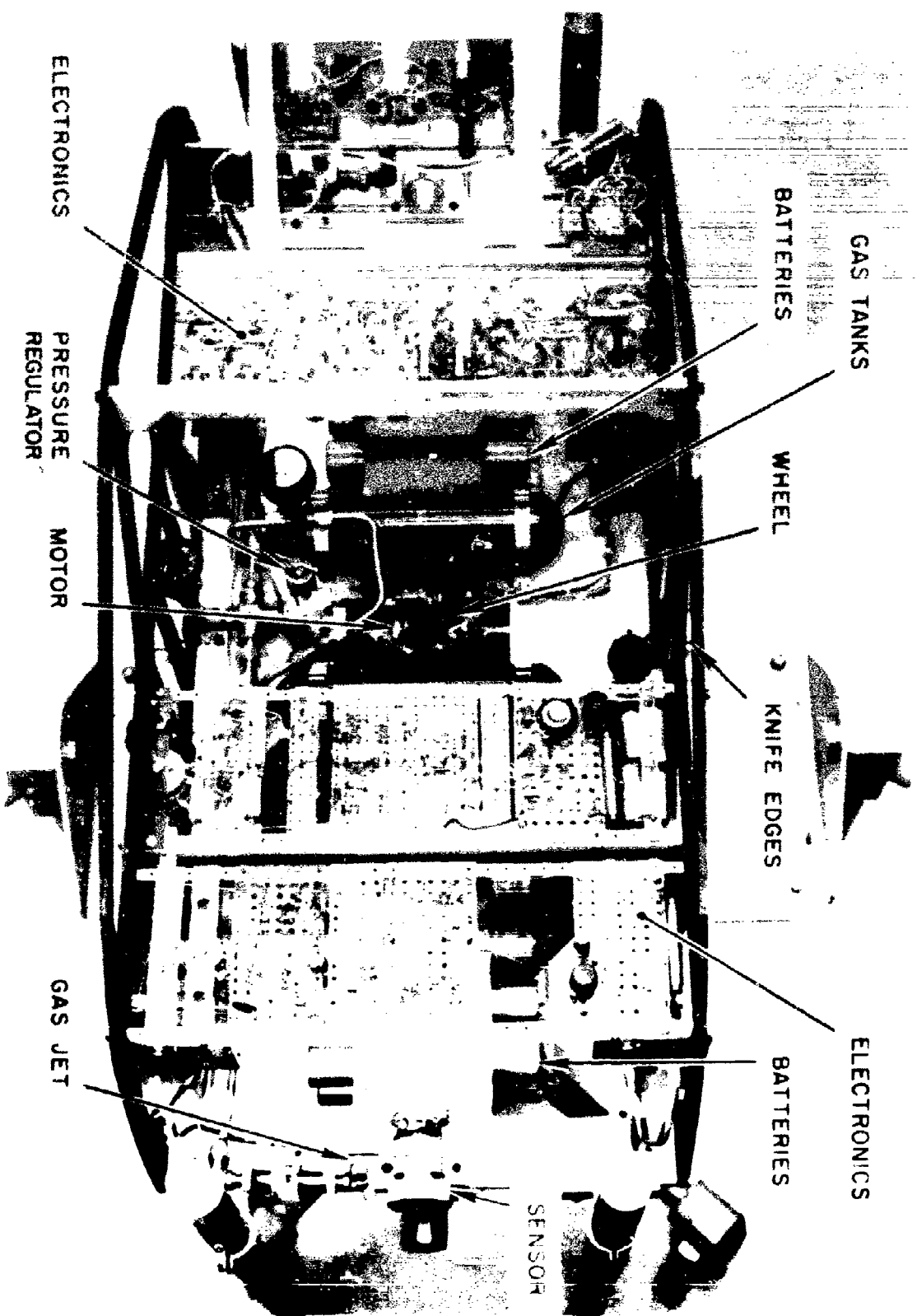
### III. THE LABORATORY MODEL

In constructing a laboratory model of a single-axis reaction wheel control system emphasis was placed upon minimizing power and weight requirement, and attaining reliable operation for at least one year. A description of the platform, the prime mover, the electronics, sensor, and the pneumatics follows (see Figure 2).



$\theta$  = ATTITUDE DEVIATION  
 $\theta_c$  = COMMANDED ATTITUDE DEVIATION  
 $\omega$  = INERTIAL WHEEL SPEED  
 $L_w$  = WHEEL CONTROL TORQUE  
 $L_J$  = GAS JET CONTROL TORQUE  
 $L_D$  = DISTURBANCE TORQUE

Figure 1. Block Diagram of Laboratory Model of Single-Axis Control System.



## **A. The Platform**

A desirable platform configuration is one in which the frictional effects of the suspension system are negligible. The methods of suspension considered were (1) the use of precision ball bearings with platform motion about a horizontal or vertical axis, (2) use of high pressure air bearings, (3) suspension vertically by wire, (4) the use of knife edges, and (5) fluid immersion. A configuration using knife edges for the bearing surfaces was chosen, giving a "teeter-totter" motion to the platform. This method of suspension was chosen because of its low frictional torque level, simplicity, and relatively short construction time. The frictional torque level of the knife edges is of the order of 0.015 oz-in., which is sufficiently low compared to the other disturbances encountered in the system. An enclosure for the platform was also added to eliminate the disturbing effects of air currents in the laboratory. Initially, the power supply and electronics were external to the platform, but the frictional effects of the interconnecting leads were not tolerable. As a result, all components including power, gas, sensor, and telemetry were mounted on the platform. To accommodate this apparatus, a platform approximately 3 feet by 1 foot was chosen, pivoted to give maximum moment of inertia.

Power on the platform was provided by Sonotone Type "X" hermetically sealed batteries, chosen to maintain platform balance during the battery's active discharge period. Hermetically sealed batteries eliminate any shift of the center of gravity of the platform due to vapor discharge or motion of liquid.

It was found that platform bending made it difficult to maintain the center of gravity of the platform exactly at the contact point of the knife edge. To remedy this situation, braces were added to make it more rigid and integration was incorporated in the control system to limit platform deviation to small angles.

## **B. The Motor**

Initial investigations were made of the specifications of all motors feasible for use in rotating the inertial wheel. The results of these investigations follow:

## 1. A-C Motors

A squirrel-cage motor does not adapt itself to speed control at zero or at low speeds without undue over-heating.

The speed of an a-c synchronous motor can be controlled by varying the frequency and amplitude of the applied voltage. In theory, this is the ideal motor for speed control. To accomplish speed control, however, it is necessary to vary the frequency and amplitude of the applied current to zero for zero speed while maintaining a constant phase shift to the motor. This can only be accomplished down to approximately 30 per cent of the full-speed values, after which excessive armature heating occurs at lower speeds. As use of this motor thus appears to be impractical, it was not included in the original studies, although it was reserved as a possibility for use at a later date.

An a-c servo motor adapts itself well to speed control, has reasonable linear torque curves over at least 80 per cent of its range, has efficiencies of about 30 per cent at maximum power output from the motor, and is readily available for testing from several manufacturers. One inherent problem with this type of motor is that excitation must be supplied to the main winding of the motor at all times when the motor is in use. To reduce this standby power to a minimum it was decided (a) that a power unbalance should exist in the servo motor to be used on the laboratory platform, and (b) that more power should be consumed in the control winding of the motor than is consumed in the main winding of the motor by a ratio of at least 4 to 1. The final ratio is dependent upon the capabilities of the amplifier system.

## 2. D-C Motors

A shunt-wound motor is well adapted to speed control, provided the field is fixed at maximum excitation and the armature voltage is varied. This type of motor always has one winding connected across the supply voltage requiring power. This motor was not entirely discounted, although it was not chosen for initial investigation.

A d-c servo motor is similar in operation to the shunt-wound motor discussed above, but exhibits better and more linear torque characteristics. It requires more power under stall conditions for the same case size,

since a d-c servo motor is, in effect, only a modified d-c shunt motor with a stronger field. If the motor were made larger, then the power required to produce the necessary flux could be reduced. This type of motor would reduce the required power in the main winding of the motor under standby conditions. As this motor leaves much to be desired from the standpoint of efficiency, it was not used.

A d-c permanent magnet motor has only one winding, good stall torque, and is more efficient than most other types of small d-c motors. As with all d-c motors, brushes could create problems at high altitudes unless the motors were hermetically sealed. It does not have linear torque curves, but is still the most promising of the regular d-c type motors. Since it is a single-winding motor, no power is required for a second winding, as in the case of the a-c motor under standby conditions. One problem inherent with any d-c motor with brushes is the inability to control running speed over a range greater than 7 or 8 to 1. However, with suitable electronics, such as a velocity servo loop, it is possible to overcome this difficulty.

An electronically commutated d-c motor using special inside-out construction techniques is presently under development and evaluation at Space Technology Laboratories, Inc. The motor is quite efficient, requires no fly-wheel (the physical rotated mass has sufficient moment of inertia) and has no brushes to cause high-altitude problems. In this motor, the position of the flux field is sensed by two balanced bridges using magneto-resistive or Hall effect in bismuth or another suitable material.

On the basis of the above considerations, a d-c permanent magnet motor, an a-c servo motor, and an electronically commutated d-c motor were chosen as possible prime movers for the wheel.

Since speed information is used in the logic functions of the system, a simple two-pole a-c permanent magnet tachometer is incorporated as an integral part of the motors to sense speed.

### C. The Electronics

Two basic speed control systems have been designed for use with the motors: (a) a 400-cps system to drive the a-c servo motor, and (b) a 10,000-cps time-modulated system to drive the permanent magnet and d-c electronically commutated motors.

#### 1. A-C Motor Power Amplifier

As system efficiencies for both the a-c and d-c motors are extremely important, it was decided to employ switching techniques to drive the motors. With these techniques, all the circuitry is either completely off and no power is dissipated in any portion of the circuit, or all the circuitry is completely on, i.e., in a condition of saturation, and the maximum possible power is delivered to the load.

In the case of the a-c motor, 400-cps square wave excitation is provided to the main winding of the motor (see Figure 3). To achieve speed control, the signal for the control winding is developed as follows.

The square wave applied to the main winding of the motor (Waveform 1, Figure 4) is integrated and amplified to provide a sawtooth waveform (see Waveform 2, Figure 4). This waveform is clamped to an appropriate level by two Zener diodes. Bias is varied on the base of the transistor to which the clamped sawtooth waveform is applied. Error voltage variation of the bias at the transistors causes amplification of only a portion of the waveform in direct proportion to the bias voltage, producing Waveform 3, Figure 4. The output signal of this stage is amplified through a high-gain amplifier to produce a square wave which varies in duration symmetrically about the  $90^\circ$  centerline (see Waveform 4, Figure 4).

This signal is then applied to a power amplifier driving the control winding. The motor is reversed by changing the polarity of the square-wave voltage applied to the main winding. A null amplifier is used to process the incoming d-c error signal to the system; the output of the null amplifier, when amplified in two Class B complimentary amplifiers, serves to change the bias level in the control amplifier circuitry.

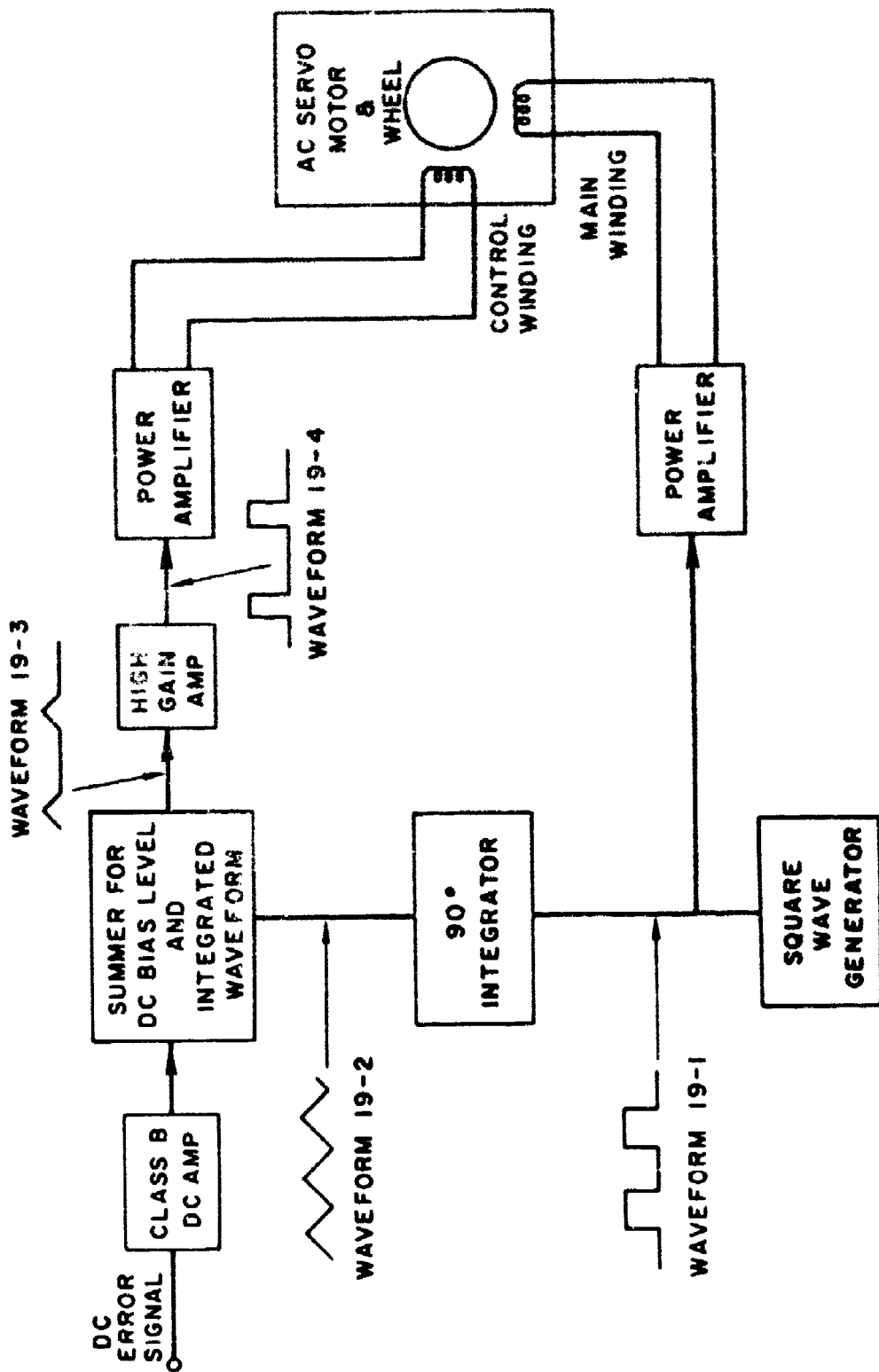
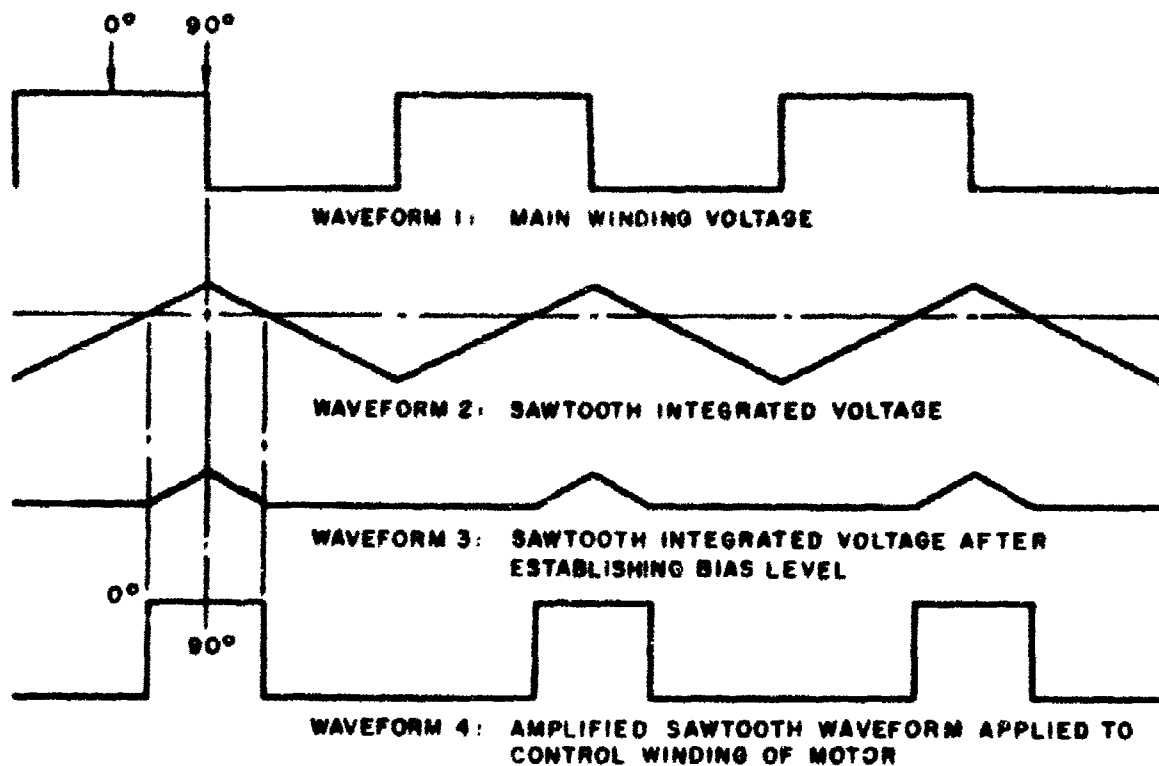


Figure 3. Block Diagram of A-C System.





1074

**Figure 4. Waveforms in Control Circuitry of A-C System.**

Several novel features have been incorporated into the a-c speed control circuitry. In order to switch the power transistors in the power amplifiers cleanly into saturation, it is necessary to have an available voltage more positive than battery voltage, since the transistors are used in an emitter-follower configuration. This voltage is obtained by means of a step-down transformer, which is connected across the 400-cps voltage supplied to the main winding of the motor. The output of this transformer feeds a full-wave rectifier and develops approximately three-fourths volt out of an r-c filter. This voltage, when added to the positive battery potential, insures that the power transistors are in a state of full saturation.

Chopper stabilization is incorporated into the null amplifier circuitry to reduce long term d-c drift. Excitation to the solid state choppers is provided by transformer coupling to the excitation supplied to the main winding of the a-c servo motor.

The square-wave generator used as a time base is a hybrid multivibrator. This three-transistor multivibrator is inherently more temperature stable than two-transistor multivibrators, as the frequency of its output is dependent only upon the temperature coefficient of one small capacitor.

The efficiency of this system, in terms of useful power delivered to the load compared to the power consumed by the amplifier is approximately 35 per cent.

## 2. D-C Motor Power Amplifier

### a. Power System

In the d-c power system, a square-wave type of controlled time-duration voltage is developed to drive both the permanent magnet and the electronically commutated d-c motors. The amplifier was designed to drive the d-c motors on the theory that if a d-c motor was pulsed at a sufficiently high frequency, the inductance of the motor winding would integrate these pulses and provide filtered d-c to the motor. Speed control would then be achieved by varying pulse width. Figure 5 is a block diagram of the d-c system.

The error signal from the attitude sensor controls the "on time,"  $T_{on}$ , of a one-shot multivibrator (see Figure 6). Another hybrid multivibrator determines the starting time for the one-shot. The output from the first hybrid and width control one-shot are summed in an AND gate. The output of the AND gate is amplified and used to drive the power amplifier connected to the motor winding. This controlled-time speed system is used for both the d-c permanent magnet and d-c electronically commutated motor.

As no 400-cps excitation is available in the d-c amplifier system, the power transistor used in the power amplifier is driven into saturation by means of a pulse current transformer. Since no excitation is available for solid-state choppers, the error signal amplifier is of complimentary symmetry design. A stable hybrid multivibrator is again used for the time base.

The efficiency of this driving amplifier in terms of power delivered to the load compared to power consumed by the amplifier is in excess of 90 per cent.

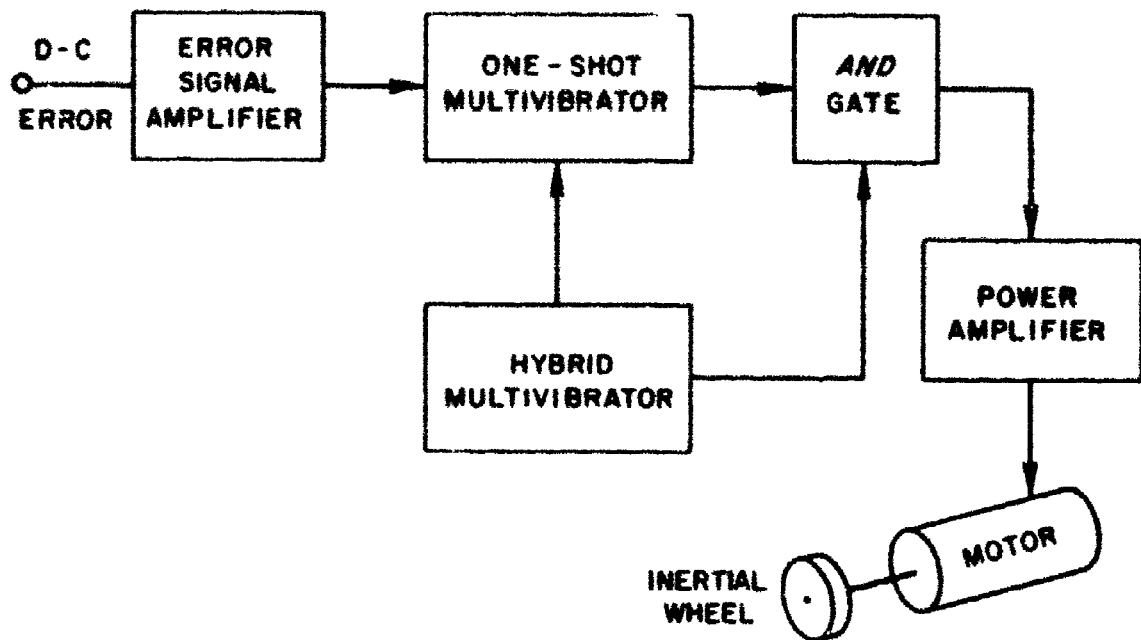


Figure 5. Block Diagram of D-C Speed Control System.

887

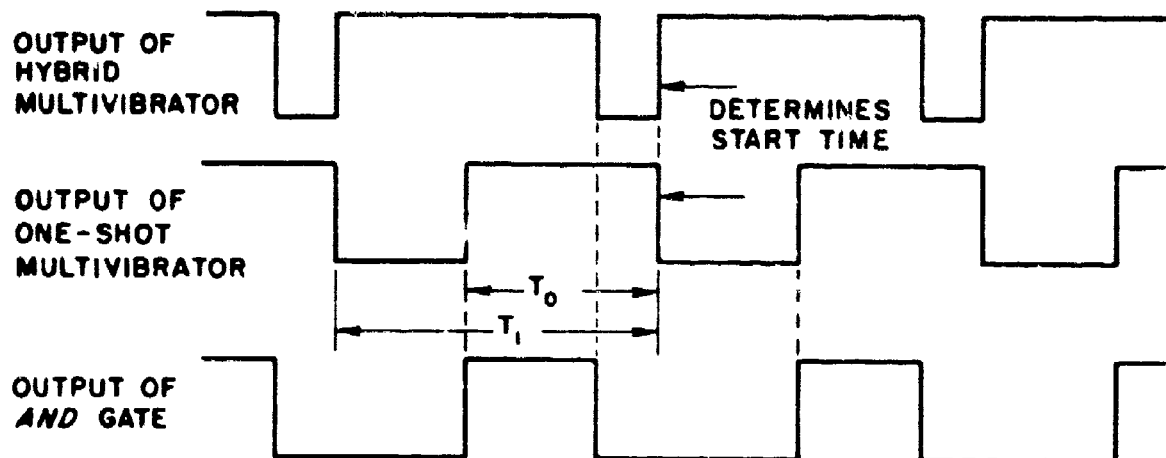


Figure 6 Essential Waveforms in the D-C System.

888

b. Commutation System

The electronically commutated motor is basically a two-winding motor. Two identical channels of electronics are used to commutate the windings. A typical channel consists of a level sensitive trigger circuit which receives its intelligence from the flux sensitive bridge that indicates the position of the flux pattern. The output of the level sensitive trigger circuit trips a flip-flop which drives a switching amplifier, connecting the proper end of the motor winding at the proper time to the correct voltage.

3. Velocity Servo Loop

Since a typical motor tested in the laboratory had an acceleration time of ten seconds from zero to maximum speed and a deceleration time of two minutes, an internal velocity servo loop was added to make system response linear. However, since the times involved in attitude control of space vehicles are on the order of several minutes rather than seconds, addition of this velocity loop may not be necessary.

The velocity servo loop incorporates a dual input photoelectric tachometer whose output, through suitable logic, supplies a voltage whose magnitude is directly proportional to the speed of the motor and whose polarity is dependent upon the direction of rotation of the motor. The output of the tachometer logic is summed with the platform error input signal, amplified by a high gain amplifier, and applied to the error signal amplifier in the power amplifier system. To provide the greatest possible stability, chopper stabilization is used in the high gain amplifier and summing portions of the servo loop.

With the addition of the velocity servo loop, both the acceleration and deceleration times of the motor are approximately ten seconds. The resulting system has better than one per cent speed linearity over its entire range.

#### D. The Sensor

To conserve power and to minimize circuitry and weight on the platform, it was decided that the input sensor should consist of: (a) a light beam placed at a convenient distance from the table to establish a reference, and (b) a visible pickup device mounted on the edge of the table to detect attitude error. Gyros are a readily available alternate which could have been used instead of the visible sensor. However, since gyros require heater power as well as three-phase excitation, a heater amplifier and a static inverter would have to be added to the platform, resulting in greatly increased battery drain, platform weight, and system complexity.

The visible sensor consists of a simple single lens which focuses the light at the rear of the cylinder (see Figure 7), where photo transistors have been mounted. The output of the sensor, either a positive or negative signal, depending on the platform's angular relationship with the incoming light rays, is amplified and used to control the associated power amplifier systems. Both position and integral feedback with lead-lag shaping are employed in the system.

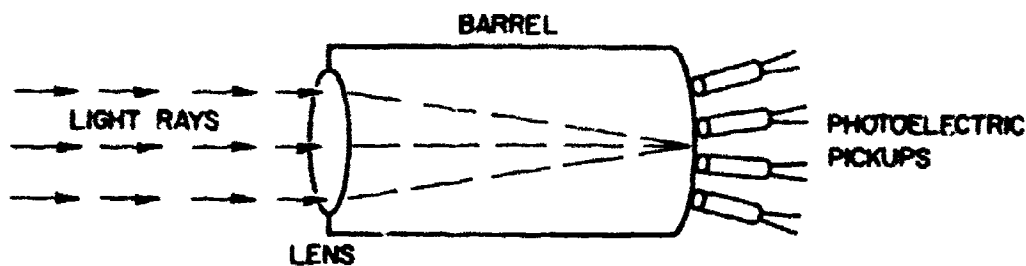


Figure 7. Mechanics of Sensor.

A simple 2-pole a-c tachometer is mounted on the motor's shaft. The output signal from the tachometer is applied across an active tuned q-multiplier circuit. The output of this circuit is an a-c frequency directly dependent upon the speed of the motor, whose amplitude has been modified by the q-multiplier. This signal is converted to a d-c voltage in a simple passive a-c to d-c circuit. This d-c clamp voltage is then used to actuate a relay, which controls the solenoid valve action in the pneumatic system of the platform. To achieve equal gas discharge times for each end of the platform, an RC time constant determines the on-time of a master relay, which actuates the appropriate slave gas solenoid valve.

### **E. The Pneumatics**

Gas is stored on the platform in four tanks whose outputs are manifolded together to maintain uniform pressure in each tank. These tanks are mounted symmetrically with respect to the center of gravity of the platform, so that no shift in the center of gravity occurs during gas discharge. The manifold output of the tanks is reduced in a two-stage pressure regulator and then piped to the solenoids mounted at the ends of the table. Figure 8 shows the gas solenoid, nozzle, and sensor mounted on the end of the table.

## **IV. GENERAL**

### **A. Reliability**

The ultimate goal in the design of this system is to achieve a high degree of reliability, and operate unattended for a period of a year or longer. The system will require little or no calibration and no selection of components, as all components are available as off-the-shelf items. Circuits have been specially designed for stability. Switching techniques keep the transistors cool and virtually no power is dissipated in the transistors because of the high circuit efficiencies, which further tend to increase the reliability of the system.

### **B. Torque, Speed, Power Relationships**

The laboratory model provided a useful stall torque of 1 oz-in., a motor speed of 12,000 rpm (before gas jet firing), and a maximum no-load speed of 20,000 rpm, while consuming approximately 9 watts of energy to maintain a constant wheel speed. The signal circuitry required to process the incoming signal requires an additional 3 to 4 watts. The system has a motor time constant of about 10 seconds for wheel acceleration from 0 to 12,000 rpm. The ratio of moment of inertia of the platform to that of the wheel was approximately 400,000 to 1. This system, with minor modifications, could be further reduced to give a 10 watt per axis system, yielding 1 oz-in. of torque.

The ultimate design goal of a system of this type would be (1) to consume no more than 10 to 15 watts for a 3-axis system, (2) to deliver torques on the order of 1/2-oz-in., with approximately the same speed capability, and

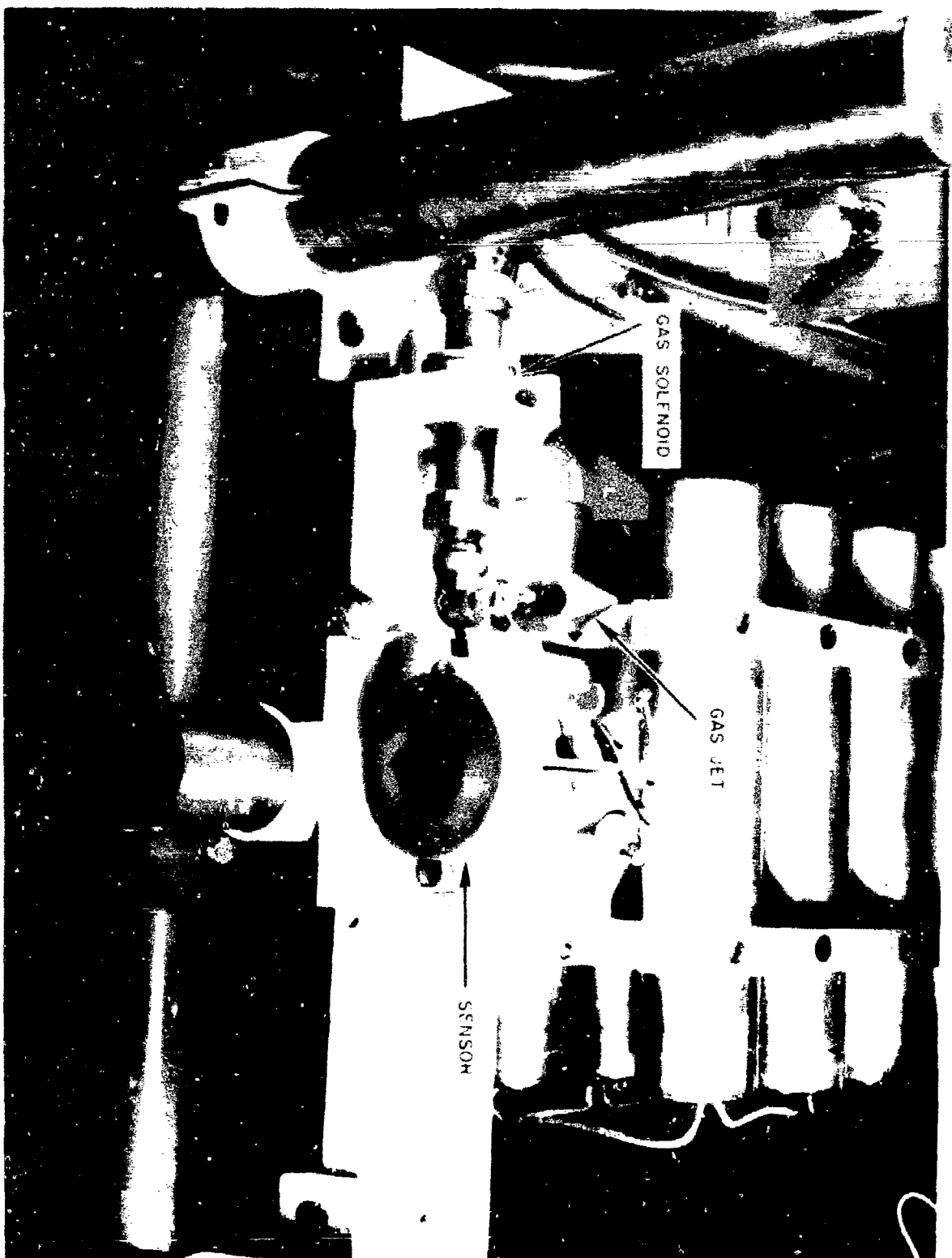


Figure 8. Gas Solenoid and Sensor Mounted on Table.

(3) to function unattended for a year or longer. The weight of this system would be no more than 10 to 15 lb. The system described in this report approaches these design goals.

#### C. Space Vehicle Control

Three-dimensional attitude control of a space vehicle can be achieved with three channels, as described above, mounted with the wheel spin axes along the vehicle principle axes of inertia. Thrust for the auxiliary mass ejection system can be generated by means of compressed gases, as in the laboratory model. Use of monopropellants or bipropellants, vaporized liquids, ion ejectors, plasma jets, etc., are also feasible for thrust generation. The control system may be simplified somewhat by eliminating the tachometer. Wheel control continues until saturation occurs, at which time any disturbance present will cause the vehicle to drift until the attitude corresponds to the dead-space value of the mass-ejection system. Firing of the jets will then drive the wheels out of saturation, where wheel control resumes.

#### D. Design Considerations

In addition to specifying attitude requirements to achieve successful operation of a specific space mission, it is necessary to have some knowledge of the causes of deviations from the desired attitude, of how such deviations can be sensed, and how they can be corrected. The gyroscopic effects of the inertial wheels must also be considered in the design of a control system. Source of disturbances, methods of sensing, and three-dimensional equations of motion are presented in the Appendix.

#### E. Selection of Control Equations

Referring to the equations of motion presented in the Appendix, it can be seen that the control problem is to make the wheel momenta, with respect to the vehicle, suitable functions of the deviations from the reference, so that resulting vehicle equations of motion have the desired stability and response characteristics. In applications where relatively large deviations in attitude can be tolerated, a control equation in which the wheel momenta are linear functions of the deviation angles and their rates may be satisfactory. Constant



wheel speeds, then, result in constant attitude errors. If attitude deviation requirements are stringent, integration can be incorporated into the control system to eliminate these errors.

Although the control equations selected for a single-axis control system may provide satisfactory performance and stability, it is by no means conclusive that three independent single-axis control channels, each a function of the corresponding deviation angle, will provide adequate performance for three-dimensional control. In the case of an orbiting vehicle in which the reference axes rotate at orbital frequency (this, in the absence of disturbances, results in a periodic transfer of momentum between wheels at orbital frequency), and in the presence of periodic disturbance torques at or near orbital frequency, stability problems may arise. More sophisticated control equations may then be necessary.

## **APPENDIX**

### **A. Disturbance Sources**

Disturbance torques which act to perturb the vehicle from the desired orientation may arise from the following sources:

- 1) Rotating parts within the vehicle.
- 2) Inertial cross-coupling due to differences in principal moments of inertia.
- 3) Interaction with ambient gravitational, magnetic, and electric fields.
- 4) Incident and emitted radiation.
- 5) Particle impingements.
- 6) Aerodynamics.

Because of present lack of knowledge of the environment to which a space vehicle will be subjected, only crude estimates of the magnitudes of disturbances can be made. It is difficult to generalize since these disturbances depend upon the vehicle configuration. The vehicle should, then, be designed to minimize these disturbing effects.

### **B. Sensing Methods**

There are a number of sensing methods that can be incorporated into a space vehicle control system. These methods can be divided into four basic classes:

- 1) Sensing by inertial means. Devices which fall into this category are gyroscopes, accelerometers, pendulums, vibrating masses, etc.
- 2) Sensing by sighting of celestial bodies. Such devices are horizon scanners, sun seekers, moon seekers, and star trackers.
- 3) Sensing by interaction with ambient fields. Such methods are quite restricted, in that ambient fields vary with altitude and orbital position. For very low altitudes use can be made of the atmospheric pressure gradient. The earth's magnetic field varies considerably with orbital position, so that some programming must be used with such a system. The observation of the differential gravitational forces on the various

parts of the vehicle requires extremely sensitive instrumentation in measuring this gravitational gradient.

- 4) Sensing by ground observation of signals transmitted from the vehicle. The field pattern of a narrow radar beam transmitted from the vehicle can yield attitude information. Correction signals are then transmitted to the vehicle from the ground station.

Although the sensing methods listed above have their limitations and disadvantages, the control designer has a relatively broad selection of feasible methods of attitude sensing.

### C. Equations of Motion

Let the reference coordinate system consist of the xyz axes, with the origin located at the center of mass of the vehicle. It is assumed, for generality, that the position of the vehicle center of mass is known as a function of time. The angular velocity  $\vec{\omega}_{\text{ref}}$  of the reference frame, then, is also known as a function of time. It has components  $\omega_x$ ,  $\omega_y$ , and  $\omega_z$  directed along the x, y, and z axes, respectively.

$$\vec{\omega}_{\text{ref}} = \omega_x \vec{e}_x + \omega_y \vec{e}_y + \omega_z \vec{e}_z \quad (1)$$

Let XYZ form an orthogonal set of body-fixed axes directed along the principal axes of inertia of the vehicle, which has principal moments of inertia  $I_X$ ,  $I_Y$ , and  $I_Z$ . The angular velocity  $\vec{\omega}_{\text{body}}$  of these body-fixed axes in inertial space has components  $\omega_X$ ,  $\omega_Y$ , and  $\omega_Z$  directed along the X, Y, and Z axes, respectively.

$$\vec{\omega}_{\text{body}} = \omega_X \vec{e}_X + \omega_Y \vec{e}_Y + \omega_Z \vec{e}_Z \quad (2)$$

Since the sensing elements will, in general, measure deviations from the reference, it may be desirable to express the body rates in terms of these deviations. The angular velocity of the reference frame, the body axes, and the angular velocity  $\vec{\omega}_{\text{rel}}$  of the body axes relative to the reference frame, are related by:

$$\vec{\omega}_{\text{body}} = \vec{\omega}_{\text{ref}} + \vec{\omega}_{\text{rel}} \quad (3)$$

Let us define these deviation angles by the three rotations,  $\theta_3$ ,  $\theta_1$ , and  $\theta_2$ , in that order, which transform the reference axes,  $xyz$ , into the body axes,  $XYZ$ .  $\theta_3$  is a rotation about the  $z$  axis, transforming  $xyz$  into  $x'y'z$ .  $\theta_1$  is a rotation about the  $x'$  axis, transforming  $x'y'z$  into  $x'Yz'$ .  $\theta_2$  is a rotation about the  $Y$  axis, transforming  $x'Yz'$  into  $XYZ$ . This sequence was selected so that  $\theta_1$  and  $\theta_2$  correspond to the gimbal angles of a gimballed "pointer" that is aligned with one of the reference axes. The choice of deviation angles, however, is arbitrary. The unit vectors in the two sets of axes are then related by:

$$\begin{pmatrix} e_X \\ e_Y \\ e_Z \end{pmatrix} = \begin{pmatrix} a_{11} & a_{12} & a_{13} \\ a_{21} & a_{22} & a_{23} \\ a_{31} & a_{32} & a_{33} \end{pmatrix} \begin{pmatrix} e_x \\ e_y \\ e_z \end{pmatrix} \quad (4)$$

where

$$a_{11} = \cos \theta_2 \cos \theta_3 - \sin \theta_1 \sin \theta_2 \sin \theta_3$$

$$a_{12} = \cos \theta_2 \sin \theta_3 + \sin \theta_1 \sin \theta_2 \cos \theta_3$$

$$a_{13} = -\cos \theta_1 \sin \theta_2$$

$$a_{21} = -\cos \theta_1 \sin \theta_3$$

$$a_{22} = \cos \theta_1 \cos \theta_3$$

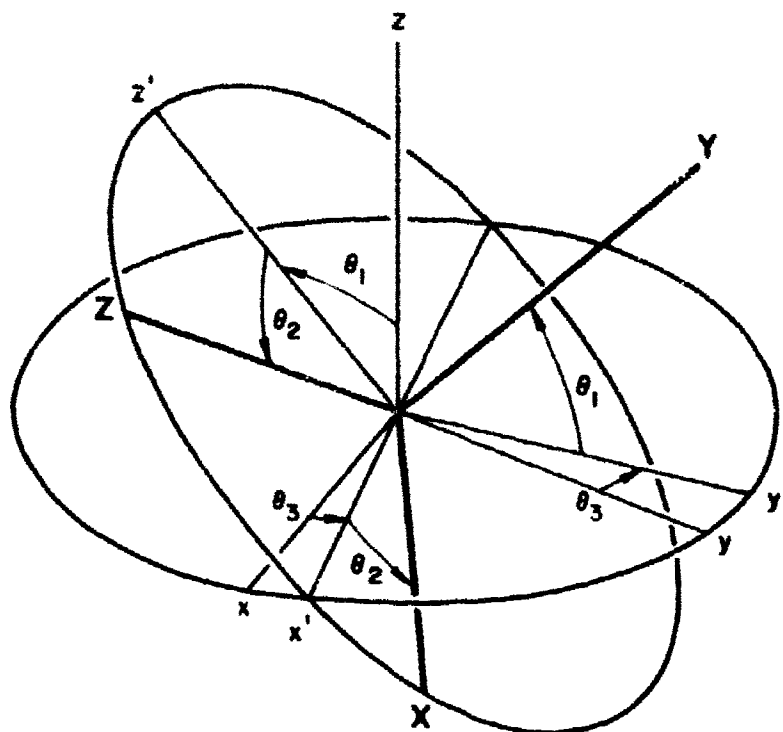
$$a_{23} = \sin \theta_1$$

$$a_{31} = \sin \theta_2 \cos \theta_3 + \sin \theta_1 \cos \theta_2 \sin \theta_3$$

$$a_{32} = \sin \theta_2 \sin \theta_3 - \sin \theta_1 \cos \theta_2 \cos \theta_3$$

$$a_{33} = \cos \theta_1 \cos \theta_2$$

This transformation is shown in diagram in Figure 9.



2567

Figure 9. Deviation Angles.

Euler's equations, which describe the general motion of a body about its center of mass, are:

$$\begin{aligned}
 I_X \dot{\omega}_X + (I_Z - I_Y) \omega_Z \omega_Y &= (L_D)_X + (L_W)_X \\
 I_Y \dot{\omega}_Y + (I_X - I_Z) \omega_X \omega_Z &= (L_D)_Y + (L_W)_Y \\
 I_Z \dot{\omega}_Z + (I_Y - I_X) \omega_Y \omega_X &= (L_D)_Z + (L_W)_Z
 \end{aligned} \tag{5}$$

where the terms on the right-hand side of equation (5) are the components of the external disturbance torque  $\bar{L}_D$  on the vehicle and  $\bar{L}_W$  the torque due to the motion of the wheels.

Using equations (3) and (4), the components of the vehicle angular velocity in inertial space directed along the body axes then become:

$$\begin{aligned}\omega_X &= a_{11}\omega_x + a_{12}\omega_y + a_{13}(\omega_z + \dot{\theta}_3) + \dot{\theta}_1 \cos \theta_2 \\ \omega_Y &= a_{21}\omega_x + a_{22}\omega_y + a_{23}(\omega_z + \dot{\theta}_3) + \dot{\theta}_2 \\ \omega_Z &= a_{31}\omega_x + a_{32}\omega_y + a_{33}(\omega_z + \dot{\theta}_3) + \dot{\theta}_1 \sin \theta_2\end{aligned}\quad (6)$$

Let  $H_X$ ,  $H_Y$ , and  $H_Z$  represent the components of the total angular momentum,  $\vec{H}$ , of the X, Y, and Z wheels relative to the vehicle frame. The torque upon the vehicle due to the motion of the wheels becomes:

$$\dot{\vec{L}}_W = -\frac{d}{dt}(H_X\vec{e}_X + H_Y\vec{e}_Y + H_Z\vec{e}_Z) \quad (7)$$

or

$$-\dot{\vec{L}}_W = \dot{H}_X\vec{e}_X + \dot{H}_Y\vec{e}_Y + \dot{H}_Z\vec{e}_Z + \vec{\omega}_{body} \times \vec{H} \quad (8)$$

The components of  $\vec{L}_W$  along the body axes are:

$$\begin{aligned}-(L_W)_X &= \dot{H}_X + H_Z\omega_Y - H_Y\omega_Z \\ -(L_W)_Y &= \dot{H}_Y + H_X\omega_Z - H_Z\omega_X \\ -(L_W)_Z &= \dot{H}_Z + H_Y\omega_X - H_X\omega_Y\end{aligned}\quad (9)$$

The general equations of motion of a vehicle with reaction wheels, then, are given by equations (5), (6) and (9). The moments of inertia of the vehicle are now defined to include the moments of inertia of the wheels. These equations are not in a form that can be suitably used for conventional control system synthesis. However, they can be reduced to a more tractable form by

linearization, so that the resulting expressions are ordinary differential equations with constant coefficients. Conventional servo techniques can then be applied.

For the single-axis laboratory model the equation of motion, excluding disturbances, is

$$I\ddot{\theta} = -\dot{H} = -J\dot{\omega} \quad (10)$$

where

$I$  = platform moment of inertia

$\theta$  = platform angular deviation

$H$  = wheel momentum

$J$  = wheel moment of inertia

$\omega$  = wheel speed

The control equation is

$$\dot{H} = \mu K_m J \frac{(s + k)(\tau_1 s + 1)}{(\tau_m s + 1)(\tau_2 s + 1)} (\theta_c - \theta) \quad (11)$$

where

$\mu$  = amplifier gain

$K_m$  = motor gain

$k$  = integrator gain

$\tau_m$  = motor time constant

$\tau_1$  = lead time constant of shaping network

$\tau_2$  = lag time constant of shaping network

$\theta_c$  = commanded platform deviation

Amplifier and integrator gains and lead-lag time constants were selected to yield a 50 per cent damped system.

## REFERENCES

1. Roberson, R.E., "Attitude Control of a Satellite Vehicle - An Outline of the Problems", presented at the Eighth International Congress of Astronautics, Barcelona, Spain, October, 1957.
2. Roberson, R.E., "Torques on a Satellite Vehicle from Internal Moving Parts", Journal of Applied Mechanics, June, 1958.